




# Geophysical Research Letters®



## RESEARCH LETTER

10.1029/2021GL096487

## The Role of Internal Variability in ITCZ Changes Over the Last Millennium

P. J. Roldán-Gómez<sup>1</sup> , J. F. González-Rouco<sup>1</sup>, C. Melo-Aguilar<sup>1</sup> , and J. E. Smerdon<sup>2</sup> 

<sup>1</sup>Instituto de Geociencias, Consejo Superior de Investigaciones Científicas - Universidad Complutense de Madrid, Madrid, Spain, <sup>2</sup>Lamont-Doherty Earth Observatory of Columbia University, Palisades, NY, USA

### Key Points:

- Last Millennium simulations contain Intertropical Convergence Zone shifts in all tropical ocean basins
- Intertropical Convergence Zone shifts in the Atlantic basin are mainly linked to changes in external radiative forcing
- Internal variability is the dominant driver of ITCZ shifts in the Pacific and Indian Ocean basins

### Supporting Information:

Supporting Information may be found in the online version of this article.

### Correspondence to:

P. J. Roldán-Gómez,  
[peroldan@ucm.es](mailto:peroldan@ucm.es)

### Citation:

Roldán-Gómez, P. J., González-Rouco, J. F., Melo-Aguilar, C., & Smerdon, J. E. (2022). The role of internal variability in ITCZ changes over the Last Millennium. *Geophysical Research Letters*, 49, e2021GL096487. <https://doi.org/10.1029/2021GL096487>

Received 12 OCT 2021  
Accepted 6 FEB 2022

**Abstract** Tropical hydroclimate is modulated by the position and intensity of the Intertropical Convergence Zone (ITCZ). Reconstructions and simulations of the Last Millennium (LM) suggest latitudinal variations of the ITCZ that impact the hydroclimate over large regions of the world. These ITCZ shifts have been generally linked to external radiative forcing, but analyses of the Community Earth System Model – Last Millennium Ensemble (CESM-LME) demonstrate a significant contribution of internal variability over multidecadal and centennial timescales. In contrast to changes driven by external forcing, which are associated with an asymmetric warming between the Northern and Southern Hemispheres, the contribution of internal variability in the CESM-LME is associated with cooling and warming of the eastern Pacific. While external forcing remains the main driver of ITCZ changes in the Atlantic basin, the contribution of internal variability in the CESM-LME exceeds that of the forcing for the Pacific and Indian Ocean basins.

**Plain Language Summary** The Intertropical Convergence Zone (ITCZ) is a wide region of increased precipitation around the Equator. The position of the ITCZ changes over time. It moves to the north during summer in the Northern Hemisphere and to the south during boreal winter. In addition to these seasonal shifts, the ITCZ also changes over longer timescales. We have used a climate model to analyze ITCZ shifts over the Last Millennium. We have found that changes in the positioning of the ITCZ over the Atlantic Ocean are mainly linked to variations in solar luminosity and volcanic events, while for the Pacific and Indian Ocean, internally driven fluctuations in atmosphere and ocean states are dominant. The understanding of the mechanisms behind ITCZ shifts allows for a better assessment of tropical hydroclimatic events, such as persistent droughts and floods that are associated with alterations in the intensity and duration of tropical monsoons, as well as for better understanding its responses under intensified climate change conditions.

## 1. Introduction

The Intertropical Convergence Zone (ITCZ), a zonal band of maximum precipitation resulting from the surface meridional convergence and convection of the tropical atmosphere, extends around the globe and stretches over the tropical regions of the Pacific, Atlantic and Indian Ocean basins (Christensen et al., 2013). The position and behavior of this band is shaped, inter alia, by the distribution of oceans and continents, with a position slightly north of the Equator over the eastern Pacific and Atlantic Oceans (Xie et al., 2007). Likewise, changes in the solar irradiance induce seasonal shifts of meridional convergence in concurrent trade winds from both hemispheres and local convection, with their northernmost and southernmost positions reached during boreal summer and winter, respectively (Huang et al., 2013). These seasonal shifts define the wet and dry seasons of many tropical areas, including the monsoon regions of Asia, Australia, the Americas, and Africa, and alterations in this seasonal cycle can produce persistent droughts and floods with important socio-economic consequences for the affected regions (IPCC, 2014).

The position and intensity of the ITCZ is known to have evolved over millennia and longer timescales as a consequence of changes in the meridional heat transport and sea surface temperatures (Donohoe et al., 2013). Southward displacements of the ITCZ have been found in simulations of the Last Glacial Maximum (LGM; Chiang et al., 2003), linked to an asymmetric cooling between the Northern Hemisphere (NH) and the Southern Hemisphere (SH) generated by a change in the amount of polar sea ice, variations in surface albedo, and changes in the Thermohaline Circulation (THC; Lohmann, 2003). This mechanism of asymmetry has been extensively analyzed in model sensitivity experiments that have investigated impacts of increased ice cover (Chiang & Bitz, 2005), NH cooling (Broccoli et al., 2006), alterations of the THC (Zhang & Delworth, 2005), and the asymmetry introduced

© 2022. The Authors.

This is an open access article under the terms of the [Creative Commons Attribution-NonCommercial-NoDerivs License](https://creativecommons.org/licenses/by-nc-nd/4.0/), which permits use and distribution in any medium, provided the original work is properly cited, the use is non-commercial and no modifications or adaptations are made.

by orography (Takahashi & Battisti, 2006). Displacements of the ITCZ are particularly relevant over oceans (Chiang & Bitz, 2005), with a northward displacement of the Pacific ITCZ in response to the cooling of the eastern Pacific (Takahashi & Battisti, 2006) or with a southward shift of the Atlantic ITCZ linked to the cooling of the northern Atlantic (Vellinga & Wood, 2002).

Changes in external forcing during the Last Millennium (LM), even if lower in magnitude than those in the LGM-to-Holocene transition, also produced significant changes in the global distribution of simulated and reconstructed temperature anomalies (Gulev et al., 2021). These radiative forcing changes also impact the simulated hydroclimate of tropical and extratropical areas (Roldán-Gómez et al., 2020), with alterations in the intensity and distribution of tropical monsoons and changes in extratropical modes of variability, like the Northern (NAM; Thompson & Wallace, 2001) and Southern Annular Modes (SAM; Fogt et al., 2009; Jones et al., 2009), coordinated with volcanic activity (Anchukaitis et al., 2010; Tejedor et al., 2021) and periods with increased or decreased temperatures like the Medieval Climate Anomaly (MCA; ca. 950–1250 CE) and the Little Ice Age (LIA; ca. 1450–1850 CE; Bird et al., 2011; Diaz et al., 2011; Graham et al., 2010).

In tropical areas, changes in external forcing like large volcanic events can induce meridional hemispheric asymmetries and trigger ITCZ shifts (Colose et al., 2016; Tejedor et al., 2021), even if the magnitude of these shifts may be relatively small and strongly depend on longitude (Atwood et al., 2020). The MCA and LIA have not been clearly associated with ITCZ shifts in simulated hydroclimate (Rojas et al., 2016), but reconstructions of precipitation for these periods show opposite behaviors between areas to the north and south of the current mean seasonal position of the ITCZ (Haug et al., 2001). In particular, reconstructions of precipitation from regions of East Africa (Brown & Johnson, 2005; Russell & Johnson, 2007) show anti-phased behavior between lakes north and south of the current ITCZ positioning during the MCA and LIA periods (Anchukaitis & Tierney, 2013). Precipitation reconstructions in the Cariaco basin, to the north of the current ITCZ, and the Peruvian Andes and the Brazil's Nordeste, to the south of current ITCZ positioning, similarly show anti-phased behavior (Novello et al., 2012; Vuille et al., 2012), as do regions of the Pacific islands (Sachs et al., 2009) and southeast Asia (Newton et al., 2006). Analyses based on reconstructed and simulated hydroclimate have suggested that this anti-phased behavior is linked to ITCZ shifts coordinated with changes in external forcing (Atwood et al., 2021; Newton et al., 2006; Sachs et al., 2009). These shifts in the ITCZ have been mostly found over the eastern Pacific and Atlantic basins, while changes in the western Pacific were more consistent with expansions and contractions of the ITCZ (Yan et al., 2015). Agreements between reconstructions and model simulations were found for the characterization of the ITCZ shifts over large areas of the Asian monsoon region, South America and the Maritime Continent, while larger differences exist in other regions, like the Pacific basin, for which the simulated hydroclimate mainly shows alterations of the Walker circulation (Atwood et al., 2021). In addition to external forcing, internal variability therefore may be important in shaping the position and intensity of the ITCZ over decades to centuries. In contrast to external radiative forcing, the role of internal variability in ITCZ changes has not been systematically analyzed.

This work assesses the contribution of internal variability on the ITCZ shifts relative to that of external forcing by analyzing simulations from the Community Earth System Model – Last Millennium Ensemble (CESM-LME; Otto-Bliesner et al., 2015). The use of an ensemble of simulations generated with the same model and different initial conditions allows for a better characterization of internal variability and external forcing contributions. We use these simulations to address the following questions:

1. Does internal variability drive ITCZ changes?
2. How does that variability compare to forced changes?
3. Is the answer to these questions dependent on the basin that is analyzed?
4. How do these results compare to proxy records?

## 2. Data and Methods

The CESM-LME (Otto-Bliesner et al., 2015) includes 13 simulations that consider natural and anthropogenic forcings using the CMIP5/PMIP3 protocol (Schmidt et al., 2011, 2012). These simulations, which span the period 850–2005 CE, are known as the “all forcing” subensemble. The external forcing considered in these simulations includes solar (Vieira et al., 2011), volcanic (Gao et al., 2008), land use (Pongratz et al. (2008) spliced to Hurtt et al. (2011) at 1500 CE), greenhouse gases (MacFarling-Meure et al., 2006), aerosols (Lamarque et al., 2010),

and orbital changes (Berger, 1978). Results from the CESM-LME have been also compared in the Supporting Information (Text S1 in Supporting Information S1) with a 3-member LM ensemble from the Goddard Institute for Space Studies (GISS; Schmidt et al., 2006; Schmidt et al., 2014) model.

Multidecadal and centennial changes in seasonal tropical precipitation have been analyzed by applying a Principal Component (PC; Barnett & Preisendorfer, 1987) analysis to intertropical precipitation. Following the approach described in Roldán-Gómez et al. (2020), the 13 simulations have been low-pass filtered with a moving average of 31 years and concatenated in a single batch, to obtain a set of Empirical Orthogonal Functions (EOFs) valid for all of them. The PC time series are obtained by projecting each individual simulation onto the EOF basis determined from the ensemble. This approach facilitates the extraction of modes of variability with a common spatial pattern for all the simulations produced with the same model. To take into account the seasonal and longitudinal variability of the ITCZ, separate analyses have been performed for the Pacific, Atlantic and Indian Ocean basins, both for the periods of December–February (DJF) and June–August (JJA).

To analyze the contribution of external forcing, common to all simulations, PC analyses have been also applied to the ensemble average. Conversely, the contribution of internal variability has been analyzed by applying the PC analyses to the concatenation of the 13 simulations after removing the ensemble average. This approach removes the common variability linked to the external forcing, while only the internal variability specific to each particular simulation is retained.

ITCZ shifts have been analyzed by computing the precipitation centroid of the area between 20°S and 20°N, except for the Pacific basin, in which the southern branch of the ITCZ (Tian & Dong, 2020) has been removed by limiting the computation to the area between 0° and 20°N. To analyze how each particular mode alters the position of the ITCZ, a comparison between the precipitation centroid in the positive and negative phases of the mode has been performed.

### 3. Results

The position of the ITCZ (Figures 1a and 1e) shows seasonal changes that are consistent with those determined by Christensen et al. (2013). In JJA, the ITCZ reaches 5°N in the Pacific and Atlantic Oceans, extends from equatorial eastern Africa over the Indian Ocean, and reaches 10°N over southern Asia. In DJF, the ITCZ shifts southward over the eastern Pacific, reaching 15°S over western South America and the Equator in the Atlantic, while in the Indian Ocean it goes from 15°S over eastern Africa to central Indonesia.

The first mode of the ensemble average shows a temporal evolution (Figures 1c and 1g) that resembles that of the external forcing, with opposite behaviors during the MCA and LIA, an impact associated with volcanic events, and a clear transition in the industrial period. According to this mode, positive net radiative forcing anomalies tend to shift the ITCZ to the south, as shown with the variations of the precipitation centroid in Figures 1b and 1f. These changes are particularly relevant in the Atlantic basin, for which shifts of 0.5° are found, but changes also appear in certain areas of the Pacific and Indian basins. Consistent with reconstructions from South America (Novello et al., 2012; Vuille et al., 2012) and Africa (Anchukaitis & Tierney, 2013), the EOF (Figures 1a and 1e) shows negative loadings north of the Atlantic ITCZ and positive loadings to the south. In the Indian Ocean basin, negative loadings are found over continental areas of India and southeast Asia and positive loadings over the ocean and in northern Australia, also consistent with southward ITCZ shifts. In the Pacific Ocean basin, ITCZ shifts are also found in DJF, but not so clearly in JJA, during which time negative loadings extend south and north of the ITCZ.

The contribution of external radiative forcing is associated with an asymmetric warming of the NH and SH, as shown in the correlations with temperature in Figures 1d and 1h. Positive correlations are found in the SH and in the high latitudes of the NH, while negative correlations spread over tropical and extratropical areas of the NH, including the northern Atlantic, northern Pacific, northern Africa, the Mediterranean basin, and regions of central Asia and eastern North America. The boundary between positive and negative correlations is found at the ITCZ location during each season, with the negative correlations reaching central Africa in DJF. This distribution of temperatures generates an asymmetry between both hemispheres that drives ITCZ shifts, similar to shifts observed in simulations of the LGM (Chiang et al., 2003) and in sensitivity experiments with increased forcings

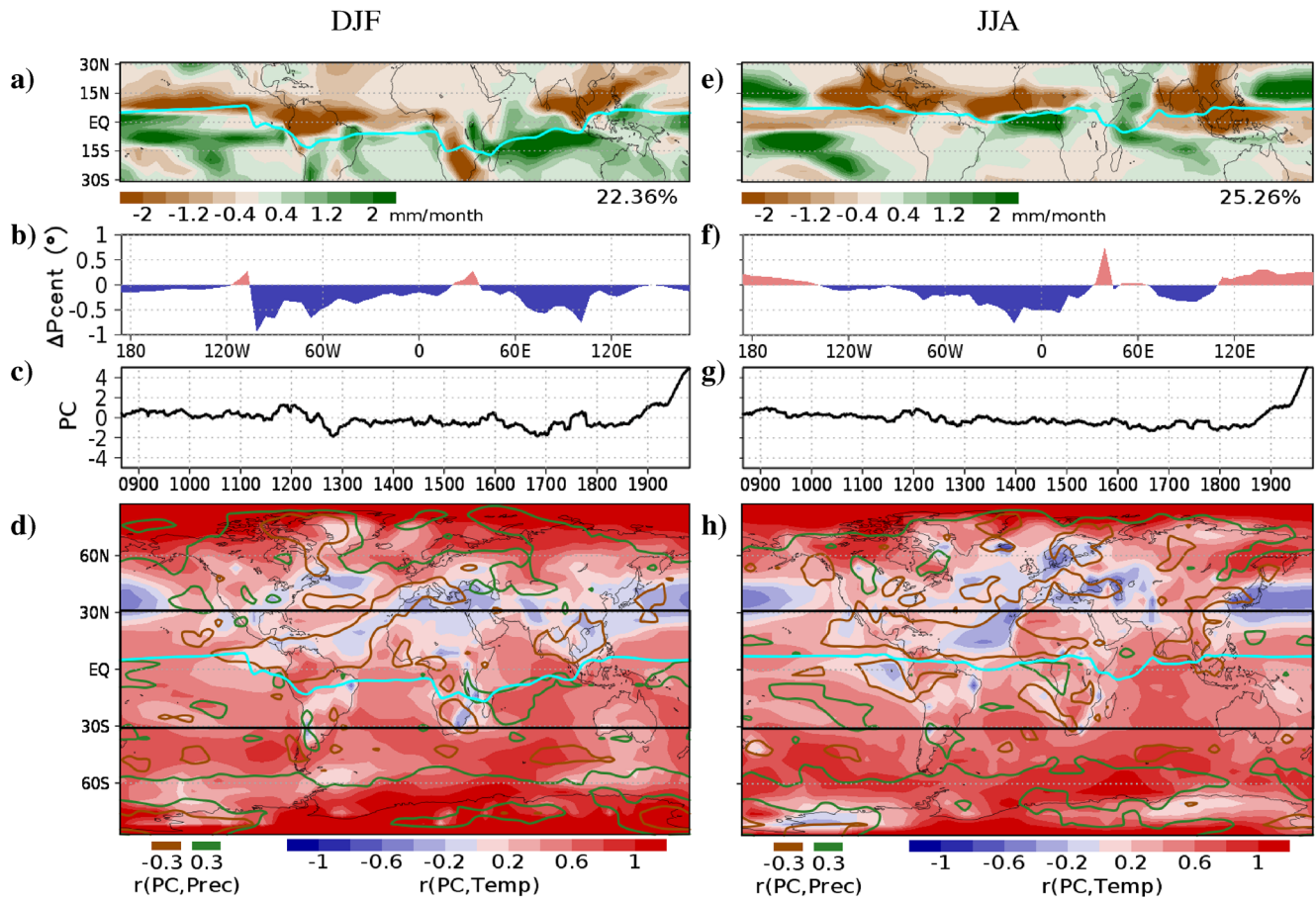


**Figure 1.** (a) First EOF of DJF tropical precipitation, obtained from the average of the “all forcing” subensemble of the CESM-LME. The percentage of explained variance is shown below the EOF map. (b) Difference between the precipitation centroid in the years with the PC greater than 1 and less than  $-1$ , expressed in degrees of latitude. (c) PC time series. (d) Correlation between temperature (shading) and precipitation (contours) and the PC time series. Horizontal black lines indicate the domain of the EOF calculation. Light blue line in panels (a) and (d) shows the tropical precipitation centroid. (e)–(h) Same as (a)–(d), but for JJA.

(Broccoli et al., 2006; Chiang & Bitz, 2005), indicating that even if variations of external forcing during the LM are smaller than those experienced during the LGM, the LGM mechanisms are also applicable to the LM.

To analyze the contribution of internal variability to ITCZ shifts, the first mode of simulated precipitation is derived, after removing the ensemble average (Figures 2a and 2e). The EOF associated with this mode shows positive loadings north of the eastern Pacific ITCZ and negative loadings to the south. This anti-phased behavior is consistent with ITCZ shifts, which in this case are driven by internal variability and are consistent with the reconstructions of precipitation from the Pacific islands (Sachs et al., 2009). The ITCZ shifts, computed as variations in the position of the precipitation centroid (Figures 2b and 2f), reach  $0.5^\circ$  for DJF and  $0.2^\circ$  for JJA. Over the Indian Ocean and the western Pacific, EOF loadings of mostly uniform sign spread over the areas of maximum precipitation, indicating that instead of shifting the ITCZ, the mode contributes to a widening of the area of maximum precipitation, in agreement with Yan et al. (2015).

In contrast to impacts from external radiative forcing, no asymmetry between the NH and SH is characterized in the correlation maps of Figures 2d and 2h. Instead, the patterns of the El Niño - Southern Oscillation and Pacific Decadal Oscillation (ENSO/PDO; Newman et al., 2016; Sarachik & Cane, 2010) appear. A regional asymmetry is found in the eastern Pacific, with positive correlations between the first mode of precipitation and temperature north of the ITCZ, and negative correlations to the south.

Shifts in the Pacific ITCZ generated by the modes of internal variability (Figures 2b and 2f) are similar in magnitude to those generated by the modes of external forcing in the Atlantic (Figures 1b and 1f), indicating that both internal variability and external forcing contribute to shape the global hydroclimate of the LM. The loadings of

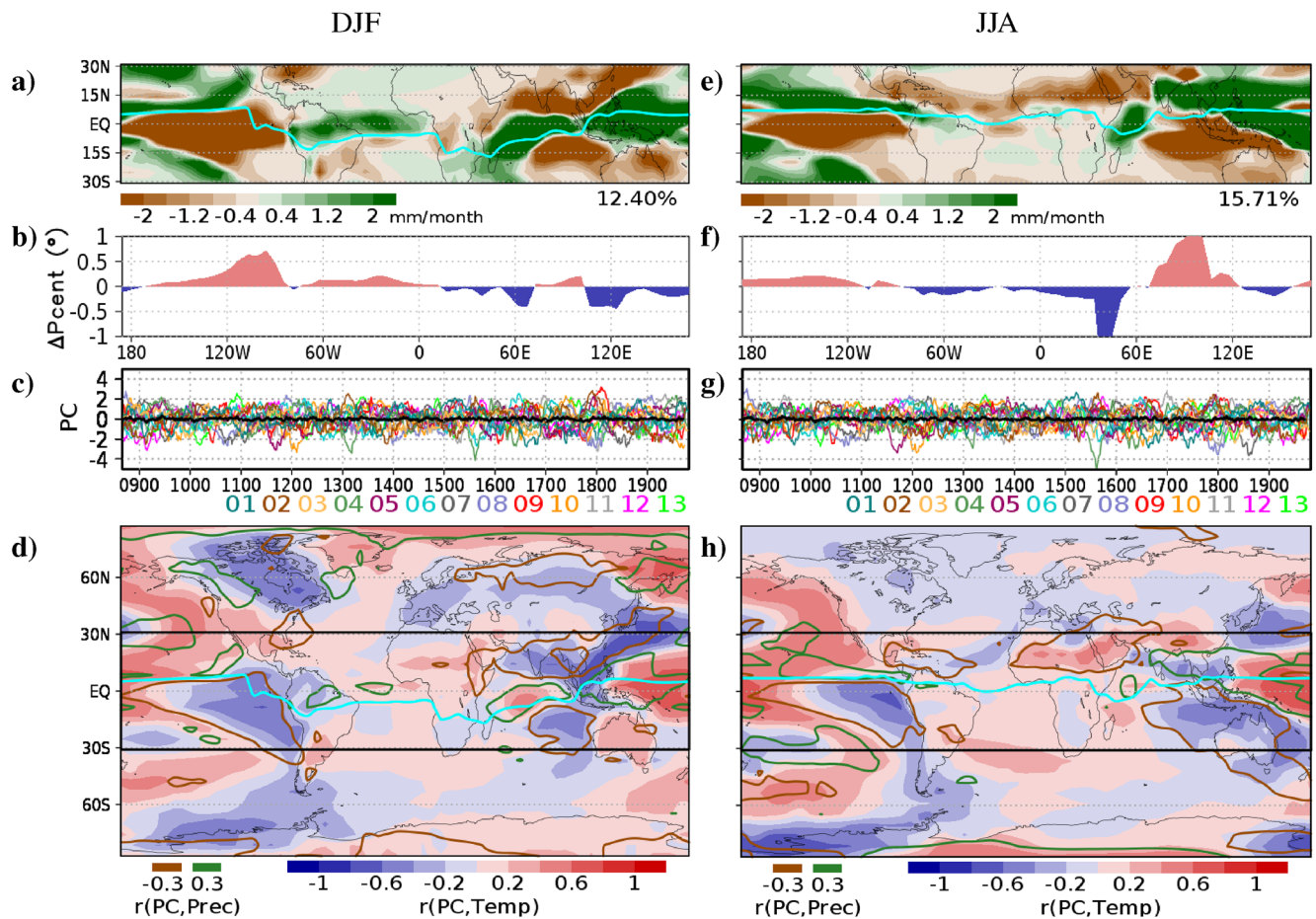


**Figure 2.** (a) First EOF of DJF tropical precipitation, obtained from the “all forcing” subensemble of the CESM-LME after removing the subensemble average. The percentage of explained variance is shown below the EOF map. (b) Difference between the precipitation centroid in the years with the PC greater than 1 and less than  $-1$ , expressed in degrees of latitude. (c) PC time series. Black line shows the average PC time series, while the colored lines are associated with the individual ensemble members. (d) Correlation between temperature (shading) and precipitation (contours) and the PC time series. Horizontal black lines indicate the domain of the EOF calculation. Light blue line in panels (a) and (d) shows the tropical precipitation centroid. (e)–(h) Same as (a)–(d), but for JJA.

the EOFs and the correlations with temperature and precipitation for the modes of internal variability (Figures 2a and 2e and 2d, 2h) also show similar magnitudes to those obtained with the modes of external forcing (Figures 1a and 1e and 1d, 1h), especially for the Pacific and Indian Ocean basins.

If the PC analysis is directly applied to the raw simulations (Figures 3a and 3d), the contributions of both external forcing and internal variability are present. The PC time series (Figures 3c and 3f) obtained for the Atlantic basin show consistent variations for all the simulations over multidecadal timescales, with a temporal evolution that corresponds to that of external forcing factors (Roldán-Gómez et al., 2020). In contrast to the results over the Atlantic, the temporal evolution shown in the leading PC time series of the Pacific and Indian basins do not present any clear signature from radiative forcing. For these basins, the forcing is instead present in the second modes (Figure S1 in Supporting Information S1). The first EOFs of precipitation within each basin account for variances that are in the range of 13%–21%, while the second modes explain less than 10% of the variance, indicating that the contribution of internal variability for the Pacific and Indian basins exceeds that of external forcing.

Over the Atlantic and the central and eastern Pacific basins, loadings of different sign indicate ITCZ shifts (Figures 3a and 3d), consistent with the phase opposition between northern and southern boundaries of the ITCZ found in reconstructions for both the Pacific (Sachs et al., 2009) and the Atlantic basins (Novello et al., 2012; Vuille et al., 2012). For the Indian and the western Pacific, positive loadings distribute over the areas of maximum precipitation and negative loadings in the boundaries, consistent with the expansions and contractions of the ITCZ shown by Yan et al. (2015). Similar patterns are obtained with the GISS model (Text S1 in Supporting

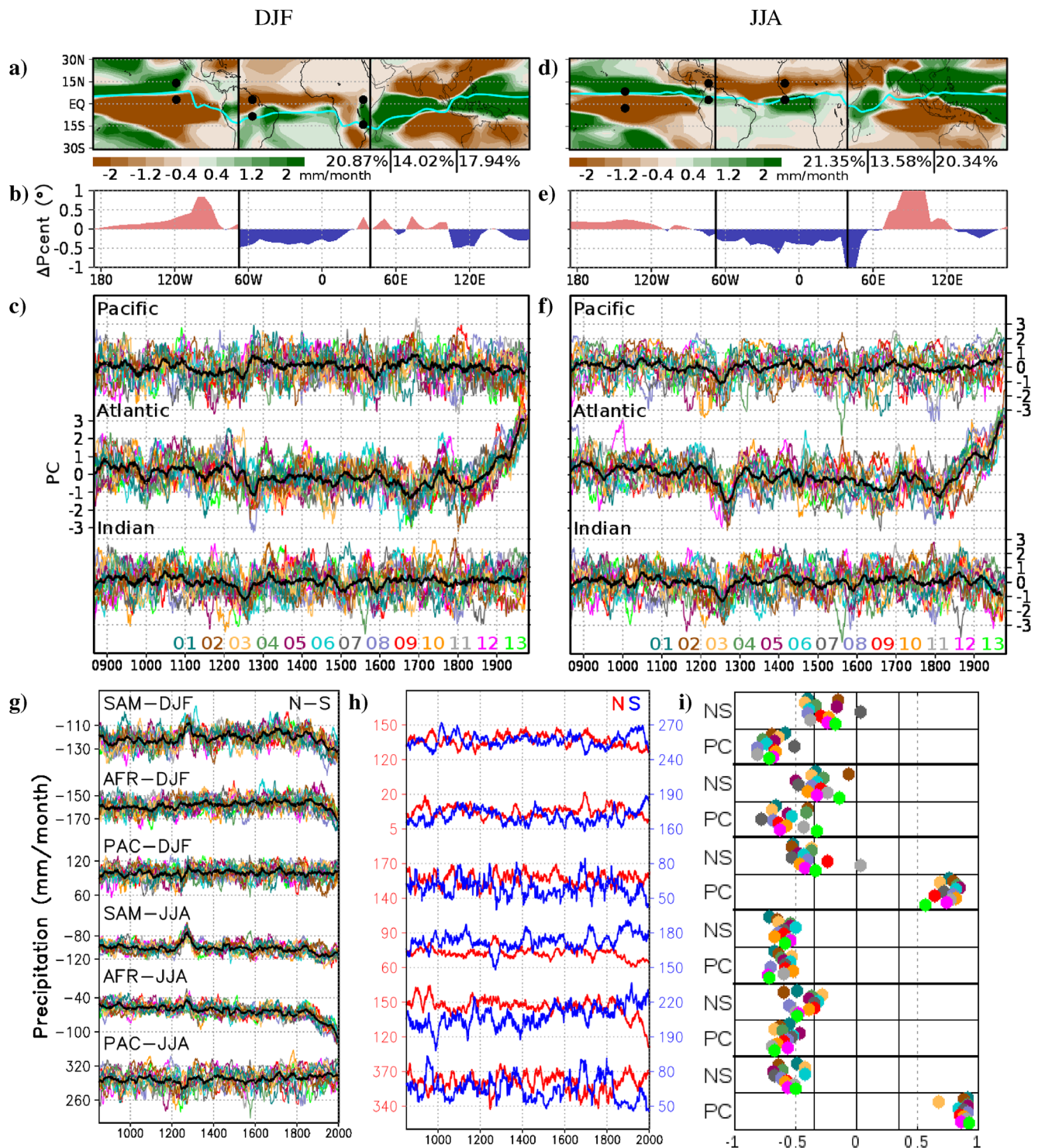


**Figure 3.** (a) First EOF of DJF tropical precipitation for the Pacific, Atlantic and Indian basins obtained from the “all forcing” subensemble of the CESM-LME. The percentage of explained variance for the three basins is shown below the EOF maps. Light blue line shows the tropical precipitation centroid. (b) Difference between the precipitation centroid in the years with the PC greater than 1 and less than  $-1$ , expressed in degrees of latitude. (c) PC time series. Black line shows the average PC time series, while the colored lines are associated with the individual ensemble members. (d)–(f) Same as (a)–(c), but for JJA. (g) Difference of precipitation between points in the North and in the South for the locations in South America (SAM), Africa (AFR), and the Pacific (PAC) represented with black dots in (a) and (d) for all the simulations of CESM-LME. Black lines show the differences for the ensemble average. (h) Time series of precipitation for the points in the North (red) and in the South (blue) for the first simulation of CESM-LME. (i) Correlations between points in the North and in the South (NS) and between the difference North-South and the PC time series of Atlantic (SAM and AFR) and Pacific (PAC) obtained with each individual simulation (PC). The significance level ( $p < 0.05$ ) accounting for autocorrelation is shown with a solid black line.

Information S1). Even if some differences exist in the results, possibly due to the smaller ensemble size, this indicates that our findings are not exclusively tied to a single model.

The changes in the position and extension of the ITCZ are illustrated by extracting time series of precipitation for locations close to the ITCZ boundaries. Locations have been selected in the Pacific, South America and Africa, in line with the reconstructions from Sachs et al. (2009), Vuille et al. (2012), Novello et al. (2012), and Anchukaitis and Tierney (2013). For all these locations, the difference between northern and southern boundaries (Figure 3g) presents a significant correlation with the PC time series (Figure 3i). This indicates that for these particular locations, the first mode shapes the evolution of precipitation and explains the anti-phased behavior found in reconstructions.

If the time series for the northern and southern boundaries of the ITCZ are separately analyzed (Figure 3h), anti-phased behaviors are observed. To avoid masking the contribution of internal variability, Figure 3h presents the time series for a single simulation. The behavior is confirmed across the full ensemble using the correlation coefficients (Figure 3i), which show negative correlations between precipitation in the northern and southern boundary regions. These negative correlations are significant for most ensemble members in JJA. In DJF, the negative correlations are not as strong, but still significant for most ensemble members in the Pacific locations and for some ensemble members in the locations of South America and Africa. For certain ensemble members, small correlations are obtained in DJF. This is the case in ensemble member 07 in South America, ensemble members 02 and 12 in locations over South America and Africa, and in ensemble member 11 for the Pacific location. A separate analysis of these simulations (Figure S2 in Supporting Information S1) shows that the anti-phased behavior between regions to the north and south of the ITCZ still exists, even if the location of the impacted areas slightly differs from the other simulations.

Similar to what is found in the modes of external forcing (Figures 1d and 1h), the Atlantic mode (Figures 4b and 4e) is indicative of weakening and strengthening of the NH latitudinal temperature gradient. Figure 4e also shows an ENSO pattern in JJA, with negative (positive) correlations with temperature over the eastern (western) equatorial Pacific. This mode could therefore link volcanic eruptions with latitudinal changes in the ITCZ and El Niño events, consistent with results from Stevenson et al. (2016) and Pausata et al. (2020). For the Pacific and Indian modes (Figures 4a and 4d and 4c, 4f), similar patterns to those obtained for the modes of internal variability (Figures 2d and 2h) are found.

#### 4. Conclusions

Our analyses show that for the LM the contribution of internal variability to ITCZ changes is as important as that of external forcing. The role of internal variability is particularly relevant over the Pacific Ocean, where it explains ITCZ shifts up to  $0.5^\circ$ , and the Indian Ocean, where it produces expansions and contractions of the ITCZ. For both basins, the contribution of internal variability is larger than that of external forcing, appearing in the first mode of variability obtained from a PC analysis and showing similarities with reconstructed data. In the Atlantic basin, even if there is also a contribution from internal variability, the tropical precipitation is mainly shaped by ITCZ shifts associated with the external forcing. Therefore, there are two types of ITCZ shifts over the LM timescale considered herein: the ones driven by external forcing, characterized by an asymmetric distribution of temperatures between the NH and SH and predominant in the Atlantic, and the ones associated with internal variability, characterized by a cooling or warming of the eastern Pacific. This behavior is likely associated with the different modes of variability involved in each basin. The strong impact of internal variability in the Pacific ITCZ is characteristic of the dynamics of ENSO/PDO, with spatial patterns showing a phase opposition between regions in the north and the south of the eastern Pacific ITCZ, while for the Atlantic, the external forcing projects on modes like the NAM and SAM.

Even if the modes associated with these ITCZ shifts only explain between 13% and 22% of the tropical variability, at the boundaries of the ITCZ these changes shape the principal characteristics of precipitation. Locations to the proximal north and south of the ITCZ in the eastern Pacific, northern and eastern South America, and central and eastern Africa show a clear anti-phased behavior in simulated precipitation, with coordinated increases and decreases. The study of the mechanisms behind these ITCZ transitions, including the impacts of internal variability and external forcing, therefore becomes a critical factor to understand the evolution of the hydroclimate in these regions.

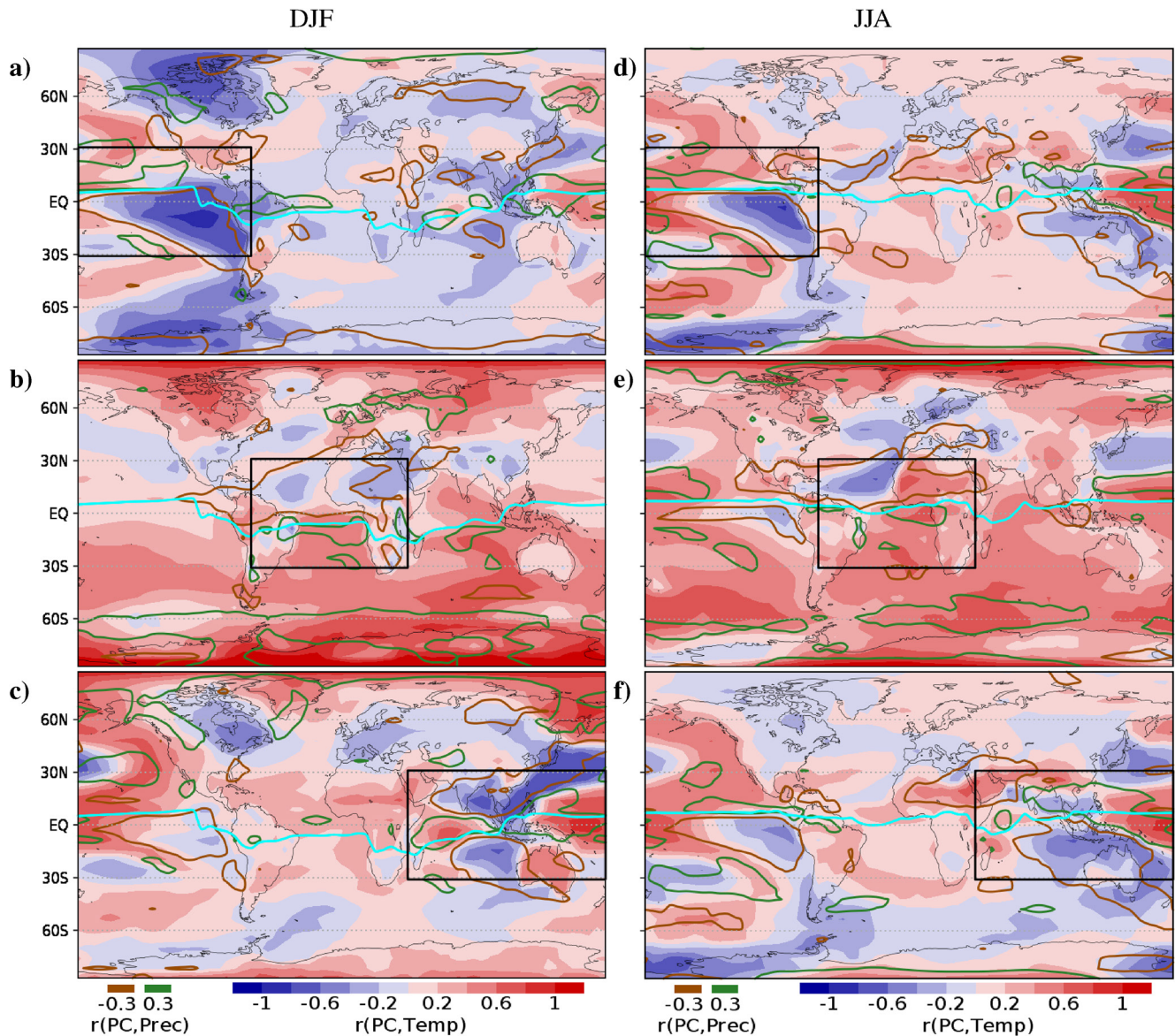


**Figure 4.** Correlation between temperature (shading) and precipitation (contours) and PC time series obtained for the areas of (a) Pacific, (b) Atlantic and (c) Indian basins (Figure 3c) for DJF. Boxes indicate the domains of the EOF calculation as in Figure 3a. Light blue line shows the tropical precipitation centroid. (d) – (f) Same as (a)–(c), but for JJA.

The relative contribution of internal variability and external forcing obtained with the CESM-LME should be confirmed with other state-of-the-art models, which may present a different characterization of internal variability and forced ITCZ responses (Text S1 in Supporting Information S1). Despite the potential differences between models, the analyses performed provide a framework for identifying which regions may be more impacted by radiative forcing, for which ITCZ transitions could be accurately characterized with model simulations, and which ones are more impacted by internal variability, for which the timing of ITCZ shifts in model simulations might be not representative of when these shifts occurred in the real world. This identification allows for a better interpretation of proxy-reconstructed shifts in ITCZ positioning over the last several millennia, and a better assessment of the risks imposed by natural variations in the ITCZ that may better characterize the hydroclimate of some tropical regions over decades to centuries.



## Data Availability Statement

The analyses included in this work have been based on the CESM-LME data, which are available in <https://www.earthsystemgrid.org/dataset/ucar.cgd.cesm4.cesmLME.html>.

## Acknowledgments

We gratefully thank the IIModels (CGL2014-59644-R) and GreatModeIS (RTI2018-102305-B-C21) projects. JES was supported in part by the US National Science Foundation grants OISE-1743738 and AGS-2101214.

## References

- Anchukaitis, K. J., Buckley, B. M., Cook, E. R., Cook, B. I., D'Arrigo, R., & Ammann, C. M. (2010). Influence of volcanic eruptions on the climate of the Asian monsoon region. *Geophysical Research Letters*, *37*, L22703. <https://doi.org/10.1029/2010gl044843>
- Anchukaitis, K. J., & Tierney, J. E. (2013). Identifying coherent spatiotemporal modes in time-uncertain proxy paleoclimate records. *Climate Dynamics*, *41*, 1291–1306. <https://doi.org/10.1007/s00382-012-1483-0>
- Atwood, A. R., Battisti, D. S., Wu, E., Frierson, D. M. W., & Sachs, J. P. (2021). Data-model comparisons of tropical hydroclimate changes over the common era. *Paleoceanography and Paleoclimatology*, *36*, e2020PA003934. <https://doi.org/10.1029/2020pa003934>
- Atwood, A. R., Donohoe, A., Battisti, D. S., Liu, X., & Pausata, F. S. R. (2020). Robust longitudinally variable responses of the ITCZ to a myriad of climate forcings. *Geophysical Research Letters*, *47*, e2020GL088833. <https://doi.org/10.1029/2020gl088833>
- Barnett, T. P., & Preisendorfer, R. (1987). Origins and levels of monthly and seasonal forecast skill for the United States surface air temperatures determined by Canonical Correlation Analysis. *Monthly Weather Review*, *115*, 1825–1850. [https://doi.org/10.1175/1520-0493\(1987\)115<1825:oaloma>2.0.co;2](https://doi.org/10.1175/1520-0493(1987)115<1825:oaloma>2.0.co;2)
- Berger, A. (1978). Long-term variations of daily insolation and Quaternary climatic changes. *Journal of the Atmospheric Sciences*, *35*, 2363–2367. [https://doi.org/10.1175/1520-0469\(1978\)035<2362:ltvodi>2.0.co;2](https://doi.org/10.1175/1520-0469(1978)035<2362:ltvodi>2.0.co;2)
- Bird, B. W., Abbott, M. B., Rodbell, D. T., & Vuille, M. (2011). Holocene tropical South American hydroclimate revealed from a decadal resolved lake sediment d18o record. *Earth and Planetary Science Letters*, *310*, 192–202. <https://doi.org/10.1016/j.epsl.2011.08.040>
- Broccoli, A. J., Dahl, K. A., & Stouffer, R. J. (2006). Response of the ITCZ to northern hemisphere cooling. *Geophysical Research Letters*, *33*, L01702. <https://doi.org/10.1029/2005gl024546>
- Brown, E. T., & Johnson, T. C. (2005). Coherence between tropical East African and south American records of the Little ice Age. *Geochemistry, Geophysics, Geosystems*, *6*, Q12005. <https://doi.org/10.1029/2005gc000959>
- Chiang, J. C. H., Biasutti, M., & Battisti, D. S. (2003). Sensitivity of the Atlantic intertropical convergence zone to last glacial maximum boundary conditions. *Paleoceanography*, *18*(NO. 4), 1094–n. <https://doi.org/10.1029/2003PA000916>
- Chiang, J. C. H., & Bitz, C. M. (2005). Influence of high latitude ice cover on the marine intertropical convergence zone. *Climate Dynamics*, *25*, 477–496. <https://doi.org/10.1007/s00382-005-0040-5>
- Christensen, J. H., Kanikicharla, K. K., Aldrian, E., An, S., Cavalcanti, I. F. A., Castro, M., & Zhou, T. (2013). Climate phenomena and their relevance for future regional climate change. In *Climate change 2013: The physical science basis. Contribution of working group I to the fifth assessment report of the intergovernmental panel on climate change*. Cambridge University Press.
- Colose, C. M., LeGrande, A. N., & Vuille, M. (2016). Hemispherically asymmetric volcanic forcing of tropical hydroclimate during the last millennium. *Earth System Dynamics*, *7*, 681–696. <https://doi.org/10.5194/esd-7-681-2016>
- Diaz, H. F., Trigo, R., Hughes, M. K., Mann, M. E., Xoplaki, E., & Barriopedro, D. (2011). Spatial and temporal characteristics of climate in Medieval Times revisited. *Bulletin of the American Meteorological Society*, *92*, 1487–1500. <https://doi.org/10.1175/bams-d-10-05003.1>
- Donohoe, A., Marshall, J., Ferreira, D., & McGehee, D. (2013). The relationship between ITCZ location and cross-equatorial atmospheric heat transport: From the seasonal cycle to the Last Glacial Maximum. *Journal of Climate*, *26*, 3597–3618. <https://doi.org/10.1175/jcli-d-12-00467.1>
- Fogt, R. L., Perlwitz, J., Monaghan, A. J., Bromwich, D. H., Jones, J. M., & Marshall, G. J. (2009). Historical SAM variability. part II: Twentieth-Century variability and trends from reconstructions, observations, and the IPCC AR4 models. *American Meteorological Society*. <https://doi.org/10.1175/2009jcli2786.1>
- Gao, C., Robock, A., & Ammann, C. (2008). Volcanic forcing of climate over the last 1500 years: An improved ice core-based index for climate models. *Journal of Geophysical Research*, *113*, D23111. <https://doi.org/10.1029/2008jd010239>
- Graham, N. E., Ammann, C. M., Fleitmann, D., Cobb, K. M., & Luterbacher, J. (2010). Support for global climate reorganization during the “Medieval climate anomaly. *Climate Dynamics*.
- Gulev, S. K., Thorne, P. W., Ahn, J., Dentener, F. J., Domingues, C. M., Gerland, S., & Vose, R. S. (2021). Changing state of the climate system. In *Climate change 2021: The physical science basis. Contribution of working group I to the sixth assessment report of the intergovernmental panel on climate change*. Cambridge University Press.
- Haug, G. H., Hughen, K. A., Sigman, D. M., Peterson, L. C., & Röhl, U. (2001). Southward migration of the intertropical convergence zone through the Holocene. *Science*, *293*, 1304–1308. <https://doi.org/10.1126/science.1059725>
- Huang, P., Xie, S. P., Hu, K., Huang, G., & Huang, R. (2013). Patterns of the seasonal response of tropical rainfall to global warming. *Nature Geoscience*, *6*, 357–361. <https://doi.org/10.1038/ngeo1792>
- Hurt, G. C., Chini, L. P., Frolking, S., Betts, R. A., Feddema, J., Fischer, G., et al. (2011). Harmonization of land-use scenarios for the period 1500–2100: 600 years of global gridded annual land-use transitions, wood harvest, and resulting secondary lands. *Climatic Change*, *109*, 117–161. <https://doi.org/10.1007/s10584-011-0153-2>
- IPCC. (2014). In V. R. Barros, C. B. Field, D. J. Dokken, M. D. Mastrandrea, K. J. Mach, T. E. Bilir, et al. (Eds.), *Climate change 2014: Impacts, adaptation, and vulnerability. Part B: Regional aspects. Contribution of working group II to the fifth assessment report of the intergovernmental panel on climate change* (p. 688). Cambridge University Press.
- Jones, J. M., Fogt, R. L., Widmann, M., Marshall, G. J., Jones, P. D., & Visbeck, M. (2009). Historical SAM variability. Part I: Century-length seasonal reconstructions. *American Meteorological Society*. <https://doi.org/10.1175/2009jcli2785.1>
- Lamarque, J. F., Bond, T. C., Eyring, V., Granier, C., Heil, A., Klimont, Z., et al. (2010). Historical (1850–2000) gridded anthropogenic and biomass burning emissions of reactive gases and aerosols: Methodology and application. *Atmospheric Chemistry and Physics*, *10*, 7017–7039. <https://doi.org/10.5194/acp-10-7017-2010>
- Lohmann, G. (2003). Atmospheric and oceanic freshwater transport during weak Atlantic overturning circulation. *Tellus*, *55A*, 438–449. <https://doi.org/10.3402/tellusa.v55i5.12108>
- MacFarling-Meure, C., Etheridge, D., Trudinger, C., Steele, P., Langenfelds, R., van Ommen, T., et al. (2006). Law Dome  $CO_2$ ,  $CH_4$  and  $N_2O$  ice core records extended to 2000 years BP. *Geophysical Research Letters*, *33*, L14810. <https://doi.org/10.1029/2006gl026152>
- Newman, M., Alexander, M. A., Ault, T. R., Cobb, K. M., Deser, C., Lorenzo, E. D., et al. (2016). The Pacific Decadal Oscillation, revisited. *Journal of Climate*, *29*(12), 4399–4427. <https://doi.org/10.1175/jcli-d-15-0508.1>

- Newton, A., Thunell, R., & Stott, L. (2006). Climate and hydrographic variability in the Indo-Pacific Warm Pool during the last millennium. *Geophysical Research Letters*, *33*, L19710. <https://doi.org/10.1029/2006gl027234>
- Novello, V. F., Cruz, F. W., Karmann, I., Burns, S. J., Strikis, N. M., Vuille, M., & Frigo, E. (2012). Multidecadal climate variability in Brazil's Nordeste during the last 3000 years based on speleothem isotope records. *Geophysical Research Letters*, *39*, L23706. <https://doi.org/10.1029/2012gl053936>
- Otto-Bliesner, B. L., Brady, E. C., Fasullo, J., Jahn, A., Landrum, L., Stevenson, S., & Strand, G. (2015). Climate variability and change since 850 C.E.: An ensemble approach with the community Earth system model (CESM). *Bulletin of the American Meteorological Society*.
- Pausata, F. S. R., Zanchettin, D., Karamperidou, C., Caballero, R., & Battisti, D. S. (2020). ITCZ shift and extratropical teleconnections drive ENSO response to volcanic eruptions. *Science Advances*, *6*, eaaz5006. <https://doi.org/10.1126/sciadv.aaz5006>
- Pongratz, J., Reick, C. H., Raddatz, T., & Claussen, M. (2008). A reconstruction of global agricultural areas and land cover for the last millennium. *Global Biogeochemical Cycles*, *22*, GB3018. <https://doi.org/10.1029/2007gb003153>
- Rojas, M., Arias, P. A., Flores-Aqueveque, V., Seth, A., & Vuille, M. (2016). The South American monsoon variability over the last millennium in climate models. *Climate of the Past*, *12*, 1681–1691. <https://doi.org/10.5194/cp-12-1681-2016>
- Roldán-Gómez, P. J., González-Rouco, J. F., Melo-Aguilar, C., & Smerdon, J. E. (2020). Dynamical and hydrological changes in climate simulations of the last millennium. *Climate of the Past*, *16*, 1285–1307. <https://doi.org/10.5194/cp-16-1285-2020>
- Russell, J. M., & Johnson, T. C. (2007). Little ice Age drought in equatorial Africa: Intertropical convergence zone migrations and El Niño - Southern Oscillation variability. *Geology*, *35*, 21–24. <https://doi.org/10.1130/g23125a.1>
- Sachs, J. P., Sachse, D., Smittenberg, R. H., Zhang, Z. H., Battisti, D. S., & Golubic, S. (2009). Southward movement of the Pacific intertropical convergence zone AD 1400-1850. *Nature Geosciences*, *2*, 519–525. <https://doi.org/10.1038/ngeo554>
- Sarachik, E. S., & Cane, M. A. (2010). *The El Niño-Southern Oscillation phenomenon*. Cambridge University Press. <https://doi.org/10.1017/CBO9780511817496>
- Schmidt, G. A., Jungclauss, J. H., Ammann, C. M., Bard, E., Braconnot, P., Crowley, T., et al. (2011). Climate forcing reconstructions for use in PMIP simulations of the Last Millennium (v1.0). *Geoscientific Model Development*, *4*, 33–45. <https://doi.org/10.5194/gmd-4-33-2011>
- Schmidt, G. A., Jungclauss, J. H., Ammann, C. M., Bard, E., Braconnot, P., Crowley, T., et al. (2012). Climate forcing reconstructions for use in PMIP simulations of the Last Millennium (v1.1). *Geoscientific Model Development*, *5*, 185–191. <https://doi.org/10.5194/gmd-5-185-2012>
- Schmidt, G. A., Kelley, M., Nazarenko, L., Ruedy, R., Russell, G. L., Aleinov, I., et al. (2014). Configuration and assessment of the GISS ModelE2 contributions to the CMIP5 archive. *Journal of Advances in Modeling Earth Systems*, *6*, 141–184. <https://doi.org/10.1002/2013ms000265>
- Schmidt, G. A., Ruedy, R., Hansen, J. E., Aleinov, I., Bell, N., Bauer, M., et al. (2006). Present day atmospheric simulations using GISS ModelE: Comparison to in-situ, satellite and reanalysis data. *Journal of Climate*, *19*, 153–192. <https://doi.org/10.1175/jcli3612.1>
- Stevenson, S., Otto-Bliesner, B., Fasullo, J., & Brady, E. (2016). “El Niño Like” hydroclimate responses to last millennium volcanic eruptions. *Journal of Climate*, *29*, 2907–2921. <https://doi.org/10.1175/jcli-d-15-0239.1>
- Takahashi, K., & Battisti, D. S. (2006). Processes controlling the mean tropical Pacific precipitation pattern. Part I: The Andes and the eastern Pacific ITCZ. *Journal of Climate*, *20*, 3434–3451.
- Tejedor, E., Steiger, N. J., Smerdon, J. E., Serrano-Notivoli, R., & Vuille, M. (2021). Global hydroclimatic response to tropical volcanic eruptions over the last millennium. *Proceedings of National Academy of Sciences*, *118*, 12, e2019145118. <https://doi.org/10.1073/pnas.2019145118>
- Thompson, D. W. J., & Wallace, J. M. (2001). Regional climate impacts of the northern hemisphere annular mode. *Science*, *293*, 85–89. <https://doi.org/10.1126/science.1058958>
- Tian, B., & Dong, X. (2020). The double-ITCZ bias in CMIP3, CMIP5, and CMIP6 models based on annual mean precipitation. *Geophysical Research Letters*, *47*, e2020GL087232. <https://doi.org/10.1029/2020gl087232>
- Vellinga, M., & Wood, R. A. (2002). Global climatic impacts of a collapse of the Atlantic thermohaline circulation. *Climatic Change*, *54*, 251–267. <https://doi.org/10.1023/a:1016168827653>
- Vieira, L. E. A., Solanki, S. K., Krivova, N. A., & Usoskin, I. (2011). Evolution of the solar irradiance during the Holocene. *Astronomy & Astrophysics*, *531*, A6. <https://doi.org/10.1051/0004-6361/201015843>
- Vuille, M., Burns, S. J., Taylor, B. L., Cruz, F. W., Bird, B. W., Abbott, M. B., & Novello, V. F. (2012). A review of the South American Monsoon history as recorded in stable isotopic proxies over the past two millennia. *Climate of the Past*. <https://doi.org/10.5194/cp-8-1309-2012>
- Xie, P., Miyama, T., Wang, Y., Xu, H., de Szoeke, S. P., Small, R. J. O., et al. (2007). A regional ocean-atmosphere model for eastern Pacific climate. *Journal of Climate*, *20*, 1504–1522. <https://doi.org/10.1175/jcli4080.1>
- Yan, H., Wei, W., Soon, W., An, Z., Zhou, W., Liu, Z., et al. (2015). Dynamics of the intertropical convergence zone over the western Pacific during the Little ice Age. *Nature Geoscience*, *8*, 315–320. <https://doi.org/10.1038/NGEO2375>
- Zhang, R., & Delworth, T. L. (2005). Simulated tropical response to a substantial weakening of the Atlantic thermohaline circulation. *Journal of Climate*, *18*, 1853–1860. <https://doi.org/10.1175/jcli3460.1>